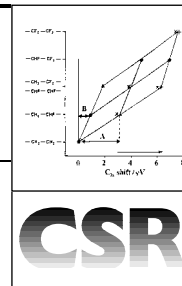


Core level photoelectron spectroscopy for polymer and catalyst characterisation



A. Paul Pijpers and Robert J. Meier

DSM Research, PO Box 18, 6160 MD Geleen, The Netherlands

Received 7th October 1998

Electron spectroscopy for chemical analysis or ESCA is a powerful tool for the characterisation of chemical species at surfaces. ESCA can therefore play a major role in the study of heterogeneous catalysts and catalytic processes. In the polymer field, more recently an increase in sensitivity combined with high spectral resolution has revealed details on the chemical environment around the probed atom. Information on nearest and next-nearest neighbours, sometimes even including conformational information, has become accessible. In catalysis the valence state of the metal centre can be estimated, and charge-binding energy relations can be used to establish charge-(catalytic) performance relations.

1 Introduction

Electron spectroscopy for chemical analysis (ESCA) has been an important analytical tool from the days it was introduced by Siegbahn and coworkers.^{1,2} The name is equivalent to what is known among physicists as X-ray photoelectron spectroscopy or XPS. The technique is about the determination of the binding energy (BE) of an electron in an atom or molecule. A key feature of the technique is its high surface sensitivity: it probes the top few nanometres of a sample from which qualitative and quantitative chemical information can be obtained. Whereas ESCA is formally core level spectroscopy only, XPS addresses both core level and valence band electron spectroscopy. In this paper we primarily limit discussion to core level spectroscopy. The reason is the straightforwardness of the interpretation of the basic features in core level spectra and the relatively high

intensities compared to valence band spectra. Moreover, for solid state samples, once the vibrational structure in the valence band spectrum is lost, the latter loses most of its significance as an analytical tool.

Siegbahn, introducing ESCA, first pointed out that chemical shifts, resulting from different chemical environments, were a general phenomenon, and the shifts can be related to the valence state of an atom. For core level spectroscopy, relative intensities of lines arising from different atoms provide direct information on their relative abundance. More recent instrumental developments in conjunction with theoretical computation of shifts in binding energy have formed the basis for the retrieval of more detailed information on the chemical environment. Examples include next-nearest neighbour induced shifts, effects due to conformational changes, and the recovery of coexisting valencies for metal ion centres. Angle resolved XPS enables depth profiling in the top 1–100 Å. These developments have further increased the significance of photoelectron spectroscopy in chemistry, mostly based on its specific surface sensitivity.

2 Theoretical background

2.1 Basic principles

The basic equation describing the photoelectron experiment is given in eqn. (1). The X-ray photon energy $h\nu$ is known by the

$$KE = h\nu - BE \quad (1)$$

source employed, the kinetic energy (KE) of the photoelectron is measured in the XPS experiment, yielding the electron binding energy (BE). However, there are complicating factors.

Paul Pijpers is a senior researcher at the DSM Research laboratories. In the period 1962–1978 he worked as an X-ray diffraction specialist. In 1978 he introduced XPS at DSM Research. In this field he is truly an autodidact. His research interests focus on the characterisation of polymers and issues

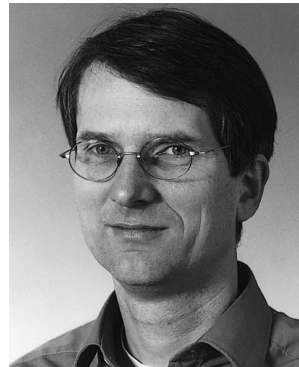
related to surface science in general, with particular attention to high resolution spectroscopy on real-life polymeric and catalytic samples in order to reveal detailed chemical information.



A. Paul Pijpers

Rob Meier is a Research Fellow in the DSM Research laboratories and an Honorary Visiting Professor in the Chemistry Department of the University of York. He studied Theoretical Chemistry at the University of Amsterdam, and graduated from the same university on a subject in condensed

matter physics. Early in 1985 he joined DSM Research where he was a group leader in Theoretical Chemistry, Raman Spectroscopy and Electron Spin Resonance. Since 1993 he has been a Research Fellow for Modelling and Spectroscopy within DSM Research, and in 1997 was given an Honorary Professorship from the University of York, UK. His main interests are computational chemistry and experimental spectroscopy.



Robert J. Meier

In an experiment on a solid, non-conducting, sample, eqn. (1) should be recast as eqn. (2), with ϕ the work function and S the

$$KE = h\nu - BE - \phi - S \quad (2)$$

sample charging effect. The work function is the energy required for the electron, when already removed from the atom on which it resided, to be taken out of the material. This involves overcoming a barrier resulting from interaction of that electron with the rest of the material. For many samples the work function lies in the range around 5 eV. It is not ultimately necessary to know the work function very accurately, for the XPS spectra can be analyzed in terms of shifts with respect to a reference signal rather than by absolute binding energies.

The precise binding energy of an electron in a molecule is determined by the net interaction of the electron with all nuclei and all other electrons. Siegbahn introduced the following description. Upon bonding of an atom and the formation of a molecule, the core level energies of the atom are influenced by the valence density on the atom as described by eqn. (3), in

$$BE = E_0 + kq \quad (3)$$

which E_0 is the electron binding energy in the isolated atom, q the valence charge, and k a proportionality constant to be determined. When a strong potential field is induced by the environment, it is necessary to add a Madelung term $\sum_{i \neq j} q_i q_j / r_{ij}$ to the right-hand-side of eqn. (3). The effect of neighbouring, chemically bonded, atoms comes from their effect on the valence electron density of the atom monitored in the XPS experiment. Different bond types lead to different effects on the valence band electron density, and thereby induce a somewhat different shift in the core level binding energy. For many cases, in particular organic systems, shifts due to various types of chemical bonds take typical values. A detailed interpretation of core level shifts can be obtained by comparing the experimental data to appropriate quantum mechanically calculated binding energies. In addition, from such calculations a relation of the form given by eqn. (3) can be established. Sets of charge–BE relations based on quantum mechanically evaluated charge values have been collected by Sleigh *et al.*,³ and may be applied to yield shifts in electron density upon variation of chemical (sub)structure.

2.2 Spectral assignment

The identification of the atom type corresponding to an observed core level binding energy is accomplished using standard tables comprising atomic core level binding energies.^{2,4,5} More detailed information can be retrieved when the precise peak position and, when present, the composition of a line profile are analyzed. As mentioned above, the chemical environment influences the BE's in a distinct pattern. Here it is useful to introduce the distinction between primary and secondary substituent effects, also referred to as nearest neighbour and next-nearest neighbour effects. Nearest neighbours often have a sizeable effect on the core level spectrum, whereas secondary shifts are usually small. A fine example of primary and secondary shifts is given by the various fluorinated polyethylenes, including polytetrafluoroethylene ("Teflon"), illustrated in Fig. 1. Fluorine is probably the element exhibiting the largest secondary shift on a next-nearest neighbouring C_{1s} level, 0.9 eV, while it induces a primary substituent effect of about 3 eV. The smaller secondary shifts induced by oxygen require high resolution, charge compensated (see Section 3), XPS spectra. Fig. 2 shows the C_{1s} XPS spectrum of poly(methyl methacrylate) (PMMA). The attribution of a secondary shift (≈ 1.0 eV) to the next-nearest neighbour effect induced by the

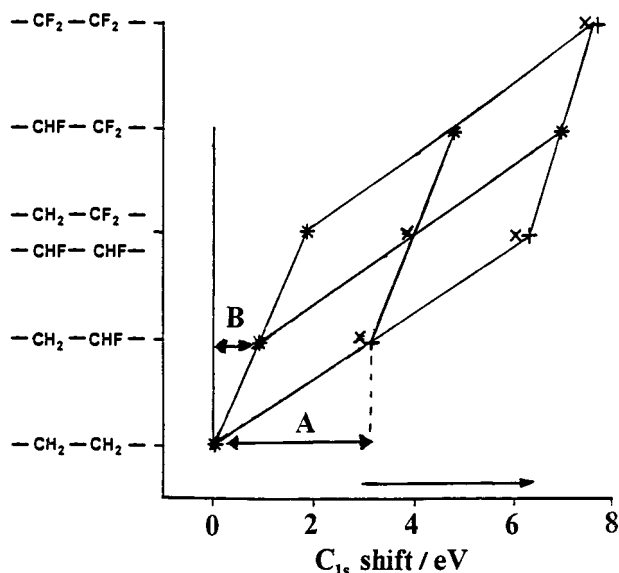


Fig. 1 Shifts in the C_{1s} binding energy due to nearest neighbour (primary shift) and next-nearest neighbour (secondary shift) effects of fluorine atoms. An example of a primary shift is indicated by A, a secondary shift by B. Experimental data from Pireaux *et al.*⁶ (+) are shown along with theoretical data (x) taken from ref. 7.

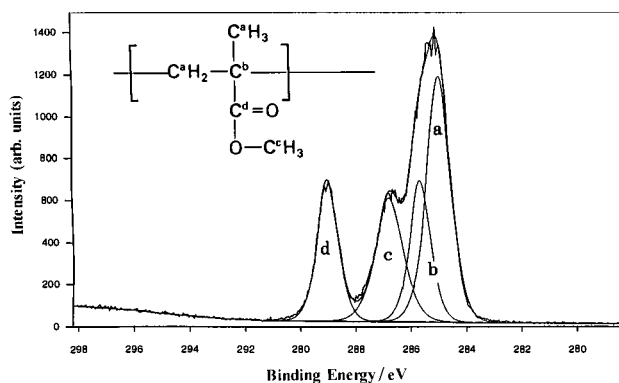


Fig. 2 C_{1s} XPS spectrum for PMMA, revealing primary ($C_{1s}-O$ and $C_{1s}(=O)O$) and secondary ($C_{1s}-C(=O)O$) shifts due to oxygen. The secondary shift is only apparent after curve fitting, but the physical significance including the magnitude of this small shift has been confirmed by theoretical calculation.

two oxygen atoms bonded to the C^b atom has been confirmed by quantum mechanical calculations.⁸

Photoexcitation of a core level may be accompanied by a valence electron excitation (shake-up) or a valence electron ionisation (shake-off). These phenomena are in fact rather common in XPS spectra, but because of their relatively low intensity are not always apparent. When present in the experimental spectrum, shake-up satellites can be used to characterise specific chemical groups. In particular for aromatic ring systems the $\pi \rightarrow \pi^*$ shake-up satellite is used for identification (*e.g.*, see the weak broad line in the range 290–292 eV in the C_{1s} spectrum of poly(ethylene terephthalate) (PET) shown in Fig. 4).

2.3 More on charge–BE energy relations

Because chemical reactivity is so much related to charge and distribution of charge, it is important to realise that charge–binding energy relations, *viz.* eqn. (3), may be applied to characterize species subjected to chemical reaction. This may

find particular use in both homogeneous and heterogeneous catalysis. Analysis of the XPS spectrum of a metal based catalyst leading to the charge on the metal centre may reveal a relevant charge–catalytic activity relation. It is, however, not *a priori* trivial to obtain the necessary charges for there is not such a thing as absolute atomic charge, except for ionised atomic species in the gas-phase. The atomic charges in a molecule may be calculated using quantum mechanical methods, but each method or level of calculation will yield a different magnitude of the charges. Apart from the level of calculation, there is an ambiguity in the way to calculate atomic charge. The charge assigned to an atom depends on how the total charge distribution in the molecule is partitioned over the atoms. The popular Mulliken analysis definitely leads to large errors for organometallics due to the complex bonding involving diffuse d- and f-orbitals. Moreover, referring to the possible application to catalytically active species, quantum chemical calculations can only be carried out on well-defined species. For this reason Folkesson and Larsson have proposed an elegant alternative.^{9,10} First, charge–BE relations are established for the elements, *e.g.* C, N and O, that comprise the ligands. Then the full XPS spectra of a series of known organometallic compounds are recorded. For each of the neutral organometallic species the charge on the metal is then assumed to have the same magnitude, but opposite sign, as the sum of charges residing on the ligands. From an analysis of the XPS spectra of the light elements, and the already established charge–BE relations for the light elements, the charge–BE relations for metal elements have been established.³

3 The XPS experiment

The basic design of a photoelectron spectrometer involves four components, illustrated in Fig. 3. First, one needs an X-ray source. Common choices are based on an Al anode with a photon energy around 1487 eV, or a Mg anode providing 1254 eV photon energy. For heavy elements the BE's for the 1s, 2s and 2p levels are much higher in energy than for light elements, and also higher than the named X-ray photon energies. Therefore one selects an appropriate set of energy levels for the various elements of the periodic table which lie within a certain range of BE's. When using either the Al-K α or the Mg-K α excitation radiation a suitable choice is given by C_{1s}, .., F_{1s}, Ti_{2p}, .., Cr_{3d}, .., Zr_{3d}, *etcetera*. When required for high resolution work, the line width of the X-ray source can be further reduced using a monochromator. The next component is the high vacuum chamber. The high vacuum is required in order to have a sufficiently long mean free path to allow the emitted photoelectrons to reach the detector, but also to keep the surface of the sample clean of any adsorbents that may otherwise contaminate the sample during handling and measurement.

In XPS, being a highly surface sensitive technique, the smallest disruption of the original surface will affect the recorded spectrum. For example, species that are sensitive to oxidation like many catalysts require a glove box with a well-conditioned atmosphere before being transferred into the high-vacuum section of the XPS-apparatus. Before the detector, the fourth component, is reached, which is usually an electron multiplier, electrons have to be selected according to their kinetic energy. This is accomplished by an analyzer, which is usually a combination of electrostatic lenses and a hemispherical analyzer. By modifying the field exerted by this lens system different electron kinetic energies are probed consecutively, providing the total photoelectron spectrum.

Some of the modern instruments allow for XPS imaging experiments.^{11,12} Imaging is a highly popular technique in optical spectroscopies. The possibility to view a spectroscopic image of a spatial domain of a material is of particular interest

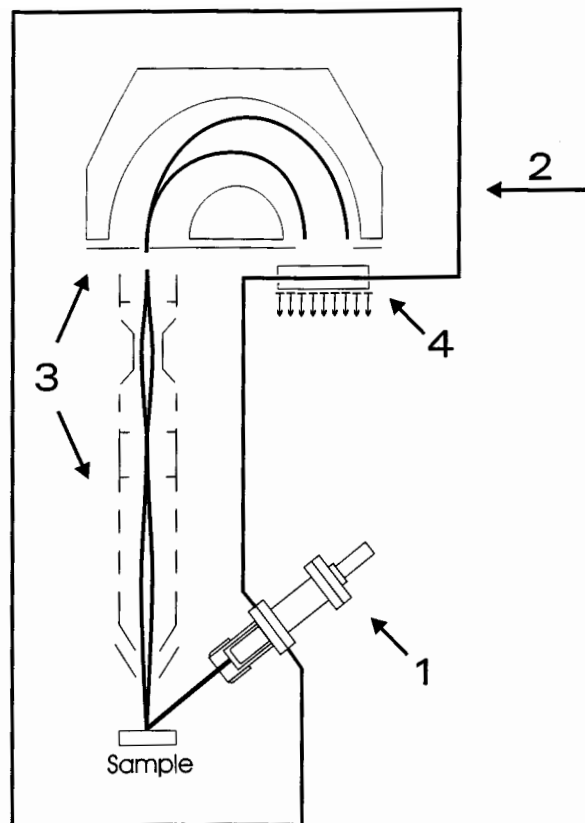


Fig. 3 Basic scheme showing the major components of an XPS instrument. The X-ray source (1), the high vacuum chamber (2), the analyzer (3) and detector (4).

to industrial applications as is well-known from micro-infrared and micro-Raman spectroscopy. We are likely to see an increase in the number of applications involving XPS imaging in forthcoming years.

The X-rays used to excite the electrons penetrate deeply into most materials. The kinetic electrons generated have, however, a limited mean free path, depending on the material and the electron kinetic energy. Because the electron kinetic energy depends on the binding energy of the probed energy level in the atom, *cf.* eqn. (1) with $h\nu$ fixed, the profiling depth may also be different for different element types in the same sample. Furthermore, the X-rays are high-energy electromagnetic radiation and may cause damage to the sample.^{4,13,14} The energy of the X-rays is much higher than the bond energy between atoms, and can thus lead to bond scission, loss of components, crosslinking and reduction. Moreover, the secondary electrons generated in the sample have a broad band energy spectrum and are therefore capable of breaking most types of chemical bonds present in the sample. In order to avoid this, a possibly low dose of X-ray photons should be applied, in combination with a sensitive detector system. When in doubt radiation damage can be monitored by following the evolution of the XPS spectrum during X-ray exposure in real time.¹³

The X-ray beam causes electrons to be removed from the atoms in the sample, leading to (positive) charging of the surface of non-conducting samples. This surface charging leads to an additional shift in the XPS spectrum, and often further broadening of the lines in the spectrum. The shift may be corrected for by considering a reference signal in the sample (see below), but the broadening may obscure valuable chemical information contained in a small shift now hidden under a broad line profile. One way to compensate surface charging is to apply a flood gun which spreads out low energy electrons homogeneously over the sample surface. A fine and more extensive discussion of the problems involved has been presented by Briggs and Seah.⁴

Effects such as surface charging and the act of a workfunction introduce an apparent shift in the BE's which is often in the order of 5 eV. In addition, there may be instrumental factors that add to this problem. The way this problem is usually tackled is to use a reference peak in the recorded spectrum. There are several possibilities in choosing a proper reference signal, e.g. the C_{1s} line from a hydrocarbon chain which has an accepted value of 284.8 eV.⁴

4 XPS applied to polymers

Much information on polymer XPS spectra is available through sources such as Briggs and Seah⁴ and Beamson and Briggs¹⁴ and Briggs.¹⁵ Over the last couple of years the higher resolution attainable with modern instruments and adequate charge compensation has allowed for the retrieval of more detail from polymer XPS spectra. Examples of polymer spectra showing next-nearest neighbour effects were shown in Figs. 1 and 2. High resolution monochromatized XPS may reveal asymmetry in line-shape due to vibrational excitation.¹⁶ XPS has been found to be extremely useful for the study of biocompatibility of polymers;¹⁷ the characterisation of apolar polymer surfaces after flame treatment (partial oxidation in order to improve adhesion properties), surface composition and surface segregation of block copolymers have been studied,^{18,19} as well as acid-base interactions in relation to adhesion.²⁰ Whereas many polymers can be discriminated using core level XPS, the important class of polyolefins poses serious problems with this technique. For this particular case valence band XPS can be used in order to distinguish between ethylene and propylene and characterize, e.g., ethylene-propylene copolymers.²¹ Apart from the study of the polymer, XPS can be employed to detect additives like release agents, lubricants and anti-statics.

Beamson *et al.*²² have reported high-resolution core level spectra of crystalline and amorphous poly(ethylene terephthalate). Spectra are shown in Fig. 4. The assignment of a

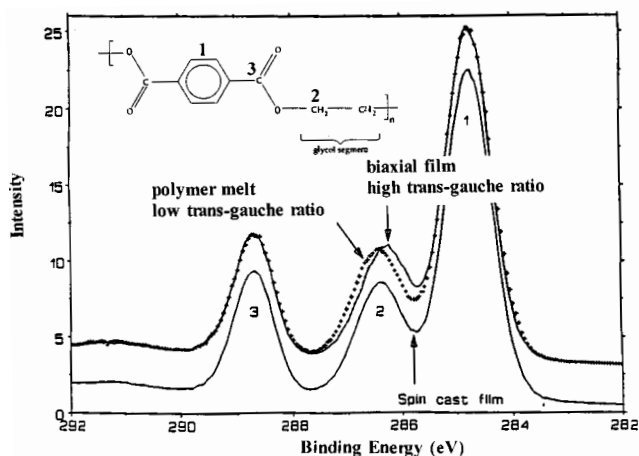


Fig. 4 Spectra from Beamson *et al.* on PET conformational dependence [Reproduced from *Polymer*, 37, G. Beamson, D. T. Clark, N. W. Hayes, D. S.-L. Law, V. Siracusa and A. Recca, p. 379, Copyright 1997, with permission from Elsevier Science].

small shift of about 0.1 eV to the *trans-gauche* difference of the glycol fragment was based on a similar shift in poly(acrylic acid) which was predicted several years ago⁸ on the basis of theoretical calculation. More recent calculations on PET have revealed²³ a theoretically predicted shift of 0.11 eV in very good agreement with the experimental shifts reported in the range 0.1–0.14 eV.

Recognising the limited escape depth of the electrons, angle-resolved XPS spectroscopy can be used to probe either the top layer of the surface or more of the bulk of the sample. When the electron take-off angle takes a small value (<10°), *i.e.* the

electrons leave almost parallel to the surface, the limited escape depth of the photoelectrons results in an extreme surface sensitivity. Fig. 5 shows C_{1s} spectra of a polymer covered with

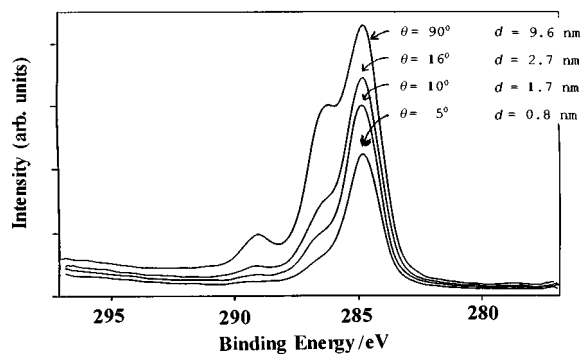


Fig. 5 Angle-resolved XPS spectra in the C_{1s} range, originating from a polymer sample coated with a very thin layer of silicon oil. The take-off values are indicated. For the lowest take-off value, surface sensitivity is highest, and only the aliphatic carbons from the silicon oil are recovered.

a thin layer of a silicon compound measured at electron take-off angles ranging between 90° and 5°. Using Mg-Kα radiation with λ = 3.2 nm, the analysis depth, obtained from $d = 3\lambda\sin\theta$, ranges from 10 nm down to less than 1 nm. The spectra clearly show the decrease of the polymer contribution at low take-off values. Analysis of these spectra allows differentiation between the signal arising from the very thin surface layer from the 5° spectrum, and the signals arising from the bulk polymer at 90° take-off angle. The “bulk” spectrum can be attributed to carbonyl and ether or alcohol functionalities, whereas the outermost layer (1 nm) is characteristic for an aliphatic group, in the present case arising from the silicon oil.

When different surface species cannot be discriminated by their straightforwardly recorded XPS spectra, e.g. because of insufficient resolution within the envelope of the peak, derivatisation of specific groups may be pursued in order to enable differentiation between the various surface groups. After treatment of the surface of apolar polymers such as polyethylene and polypropylene by flame or plasma with the objective to incorporate oxygen at the surface in order to improve adhesive properties, it is not possible to discriminate an ether from an epoxide or an alcohol since all carbons and oxygens present in C–O bonds exhibit mutually minor differences in core level BE's. Derivatisation with a reactant which is selective with respect to one of the functionalities allows for discrimination in the XPS spectrum. An example is illustrated in Fig. 6, showing the result of treating the alcohol functionality in polyvinyl alcohol by trifluoroacetic acid (eqn. (4)). The overview XPS



spectra shown in Fig. 6 show that the alcohol function is very well accounted for by the strong fluorine related signal in the derivatised sample. Several studies have been presented, though the method is not without pitfalls,^{16,24} in particular with respect to the chemistry involved in derivatisation. In particular the efficiency of the reactions and the occurrence of side reactions require attention.

5 XPS applied to catalysis

The potential application of ESCA to catalysis involving metal containing compounds has been known for quite some time.^{25,26} Application was demonstrated to both homogeneous and heterogeneous catalysis. Correlations between acidity/basicity and XPS shifts have been reported.^{27,28} Like for polymers, more recently higher spectral resolution has enabled more detailed

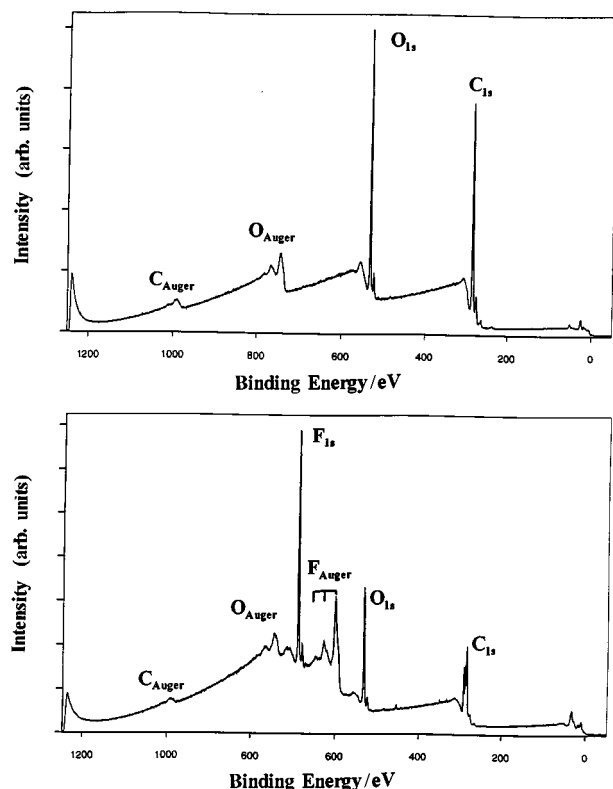


Fig. 6 XPS overview spectra showing the change when an alcohol functionality is derivatised with trifluoroacetic acid. The upper spectrum originates from polyvinyl alcohol, the lower spectrum from the same sample after treatment with trifluoroacetic acid. The specificity of the derivatisation which is accompanied by the introduction of a clearly visible fluorine related line allows for the specific detection of the alcohol functionality.

assignments. Angle resolved studies on dispersed catalysts on support, *e.g.* silica support, showed that the dispersed catalyst centres are really located at the surface.²⁹

Olefin polymerisation catalysts of the metallocene type are of huge contemporary interest, both academically as well as industrially. A simple model system is the biscyclopentadienyl zirconium species $Zr(C_5Me_5)_2Me_2$ which requires activation in order to yield the active catalyst $Zr(C_5Me_5)_2Me^+$. The XPS spectrum of the neutral starting complex shows the typical $Zr\ 3d_{3/2}-Zr\ 3d_{5/2}$ doublet with these components separated by 2.2 eV. After activation a shift of the $Zr\ 3d$ BE of about 1 eV was observed, which is of the correct magnitude expected for a +1 change in formal charge.

The well-known Phillips catalyst for olefin polymerisation involves chromium dispersed on silica. From the chemistry it seems unlikely that $Cr(II)$ and bulk $Cr(VI)$ are stable under calcination conditions, whereas signals due to isolated $Cr(VI)$, isolated $Cr(III)$ and bulk $Cr(III)_2O_3$ may be expected. Isolated here means that the Cr is linked, *via* an oxygen bridge, to a silicon atom rather than to another Cr as in bulk chromate. The Cr_{2p} region in the XPS of some calcined samples are shown in Fig. 7a. The lower spectrum shows the characteristic doublet ($2p_{1/2}$, $2p_{3/2}$) of isolated $Cr(VI)$ on silica. In the upper spectrum another doublet is visible with its $2p_{3/2}$ component at 575.8 eV, which can be attributed to bulk $Cr(III)$. Curve fitting, however, shows at least one more component is present. This component might be either bulk $Cr(VI)$ or isolated $Cr(III)$ on silica, a hypothesis which can be tested assuming an analogy with secondary substituent effects in polymers. For this particular case we have verified by quantum mechanical calculations applied to the models depicted in Fig. 7b, that indeed there is a next-nearest neighbour effect on the Cr_{2p} BE of 2.0 eV, which compares very well to the experimental difference of 2.1 eV (Fig. 7a) between the (fitted) peaks at 581.6 ± 0.1 eV (isolated

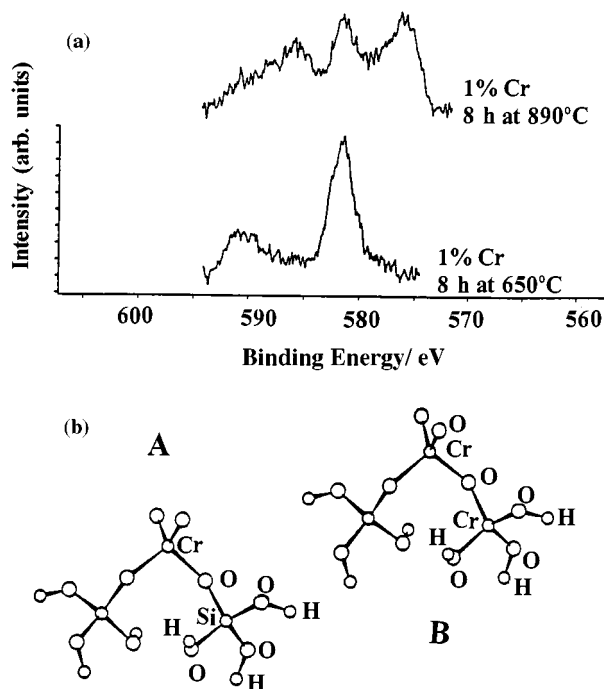


Fig. 7 (a) Cr_{2p} region of the XPS spectrum of a calcined Phillips catalyst sample. (b) Models for $Cr(VI)$ bulk and $Cr(VI)$ on silica studied by quantum mechanical calculation to reveal the difference in $2p$ BE's.

$Cr(VI)$) and 579.5 ± 0.5 eV (bulk $Cr(VI)$) in the experimental spectra of the shown and other Cr-on-silica samples.

XPS spectra of pure metal surfaces recorded at sufficiently high resolution may show differences between the surface core level shifts and the bulk atom shift.³⁰ An example is shown in Fig. 8, showing decomposition of the $Pd\ 3d_{5/2}$ core level into

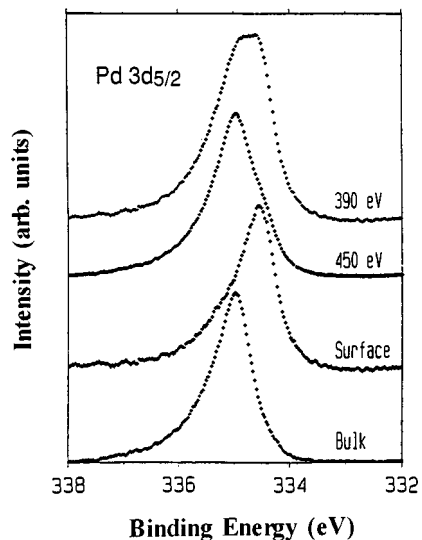


Fig. 8 Decomposition of the $Pd\ 3d_{5/2}$ core level into bulk and surface components [Reproduced from *J. Phys.: Condens. Matter*, **4**, R. Nyholm, M. Quarford, J. N. Andersen, S. L. Sorensen and C. Wigren, p. 277, Copyright 1992, with permission from IOP Publishing Limited].

bulk and surface atom components. This decomposition could be physically justified by varying the excitation energy (390 and 450 eV, respectively), which causes a variation in the ratio between contributions from surface and bulk Pd atoms as a result of the change in escape depth as a function of electron kinetic energy (see the upper two spectra in Fig. 8). The surface character of one of the peaks in the decomposition was further substantiated by showing that the presence of adsorbates on the

Pd surface made this peak disappear, and by theoretical support.

The vibrational fine structure and orientation of ethylene and ethynidyne on Rh(111) have been studied³² by monitoring the C_{1s} spectra of C₂H₃ and C₂D₃ overlayers on the Rh substrate, see Fig. 9. In order to reduce broadening due to low energy

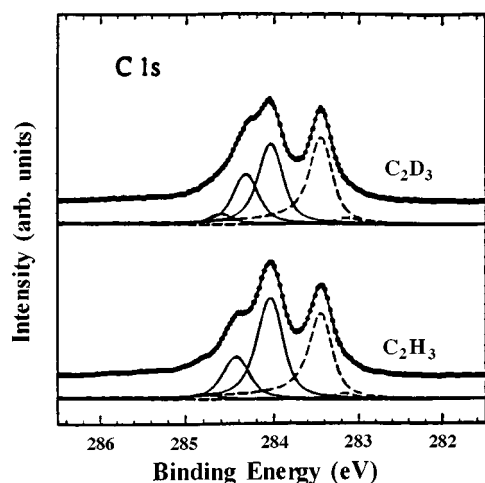


Fig. 9 C_{1s} XPS spectra from Rh(111)-C₂H₃ and C₂D₃ overlayers. Dots represent experimental data points, the thinner (broken) lines are results from curve fitting [Reproduced from *Chem. Phys. Lett.*, **269**, J. N. Andersen, A. Beutler, S. L. Sorensen, R. Nyholm, B. Setlik and D. Heskett, p. 371, Copyright 1997, with permission from Elsevier Science].

vibrational excitations, all measurements were carried out at 100 K. The existence of two main peaks is consistent with the upright geometry of the adsorbate molecule, a feature which was independently found from a quantitative LEED (low energy electron diffraction) study. In addition, the C₂H₃ spectrum shows at least two shoulders on the high binding energy side, whereas in the C₂D₃ spectrum the first shoulder has moved considerably closer to the main peak and the second peak is hardly discernable. The combination of these observations leads to the interpretation of C–H vibrational fine structure in these C_{1s} spectra. It should be emphasized that the vibrational energy involved is that corresponding to the core ionised molecule, and thus cannot be interpreted on the basis of frequencies known from traditional infrared or Raman vibrational spectroscopy.

6 References

- 1 K. Siegbahn, C. Nordling, G. Johansson, J. Hedman, P. F. Heden, K. Hamrin, U. Gelius, T. Bergmark, L. O. Werne, R. Manne and Y. Baer, *ESCA Applied to Free Molecules*, 1969, North-Holland Publishing Company, Amsterdam, London.
- 2 K. Siegbahn, C. Nordling, A. Fahlman, R. Nordberg, K. Hamrin, J. Hedman, G. Johansson, T. Bergmark, S. E. Karlsson, I. Lindgren and B.

- Lindberg, *ESCA - Atomic, Molecular and Solid State Structure Studied by Means of Electron Spectroscopy*, Uppsala, 1967. *Nova Acta Regiae Soc. Sci. Ups. Ser. IV*, **20**, 1967.
- 3 C. Sleight, A. P. Pijpers, A. Jaspers, B. Coussens and R. J. Meier, *J. Electron Spectrosc. Relat. Phenom.*, 1996, **77**, 41.
- 4 D. Briggs and M. P. Seah, *Practical Surface Analysis*, vol. 1, 2nd edn., Wiley, Chichester, 1990.
- 5 W. L. Jolly, K. D. Bomben and C. J. Eyermann, *At. Nucl. Data Tables*, 1984, **31**, 433.
- 6 J. J. Pireaux, J. Riga, R. Caudano, J. J. Verbist, J. M. Andre, J. Delhalle and S. Delhalle, *J. Electron Spectrosc. Relat. Phenom.*, 1974, **5**, 531.
- 7 R. J. Meier, *J. Mol. Struct. (THEOCHEM)*, 1988, **181**, 81.
- 8 R. J. Meier and A. P. Pijpers, *Theor. Chim. Acta*, 1989, **75**, 261.
- 9 P. Sundberg, C. Andersson, B. Folkesson and R. Larsson, *J. Electron Spectrosc. Relat. Phenom.*, 1988, **46**, 85.
- 10 B. Folkesson and R. Larsson, *J. Electron Spectrosc. Relat. Phenom.*, 1990, **50**, 267.
- 11 M. Keenlyside and P. Pianetta, *J. Electron Spectrosc. Relat. Phenom.*, 1993, **66**, 189.
- 12 C. Coluzza and R. Moburg, *J. Electron Spectrosc. Relat. Phenom.*, 1997, **84**, 109.
- 13 A. P. Pijpers, in *Scientific Methods for the Study of Polymer Colloids and their Applications*, eds. F. Candau and R. H. Ottewill, Kluwer Academic Publishers, 1990, p. 291.
- 14 G. Beamson and D. Briggs, *High Resolution XPS of Organic Polymers: The Scienta ESCA300 Database*, 1992, Wiley, Chichester.
- 15 D. Briggs, *Surface Analysis of Polymers by XPS and Static SIMS*, Cambridge University Press, Cambridge, 1998.
- 16 G. Beamson, D. T. Clark, J. Kendrick and D. Briggs, *J. Electron Spectrosc. Relat. Phenom.*, 1991, **57**, 79.
- 17 L. Sabbatini and P. G. Zambonin, *J. Electron Spectrosc. Relat. Phenom.*, 1996, **81**, 285.
- 18 C. M. Kassis, J. K. Steehler, D. E. Betts, Z. Guan, T. J. Romack, J. M. DeSimone and R. W. Linton, *Macromolecules*, 1996, **29**, 3247.
- 19 L. Li, C.-M. Chan and L. T. Weng, *Macromolecules*, 1997, **30**, 3698.
- 20 S. R. Leadly and J. F. Watts, *Polymer-Solid Interfaces: from Model to Real Systems*, ICPSI-2, Proceedings of the Second International Conference, eds. J.-J. Pireaux, J. Delhalle and P. Rudolf, Presses Universitaires de Namur, 1998.
- 21 A. A. Galuska and D. E. Halverson, *Surf. Interface Anal.*, 1998, **26**, 425.
- 22 G. Beamson, D. T. Clark, N. W. Hayes, D. S.-L. Law, V. Siracusa and A. Recca, *Polymer*, 1996, **37**, 379.
- 23 A. Tarazona, E. Koglin, A. P. Pijpers and R. J. Meier, *Polymer*, 1997, **38**, 2615.
- 24 C. D. Batich, *Appl. Surf. Sci.*, 1988, **32**, 57.
- 25 *New Catalytic Materials: Volume XI. State-of-the-art techniques for catalyst characterisation*, 1984, Catalytica Associates, Inc., California, USA.
- 26 S. C. Avanzino, H.-W. Chen, C. J. Donahue and W. L. Jolly, *Inorg. Chem.*, 1980, **19**, 2201.
- 27 M. Casamassima, E. Darque-Ceretti, A. Etcheberry and M. Aucouturier, *J. Mater. Sci.*, 1993, **28**, 3997.
- 28 H. J. M. Bosman, A. P. Pijpers and A. W. M. A. Jaspers, *J. Catal.*, 1996, **161**, 551.
- 29 F. Verpoort, A. R. Bossuyt and L. Verdonck, *J. Electron Spectrosc. Relat. Phenom.*, 1996, **82**, 151.
- 30 J. N. Anderson, D. Hennig, E. Lundgren, M. Methfessel, R. Nyholm and M. Scheffler, *Phys. Rev. B*, 1994, **50**, 17525.
- 31 R. Nyholm, M. Qvarford, J. N. Andersen, S. L. Sorensen and C. Wigren, *J. Phys.: Condens. Matter*, 1992, **4**, 277.
- 32 J. N. Andersen, A. Beutler, S. L. Sorensen, R. Nyholm, B. Setlik and D. Heskett, *Chem. Phys. Lett.*, 1997, **269**, 371.

Review 8/07826B